Model of luminescence and delayed luminescence correlated blinking in single $CsPbBr_3$ nanocrystals. Supplementary Notes.

Eduard A. Podshivaylov[1], Alexandr M. Shekhin[1], Maria A. Kniazeva[2,3], Alexander O. Tarasevich[3], Elizaveta V. Sapozhnikova[4], Anatoly P. Pushkarev[5], Ivan Yu. Eremchev[6], Andrei V. Naumov[3,6,7], and Pavel A. Frantsuzov[1,*]

[1]Voevodsky Institute of Chemical Kinetics and Combustion SB RAS, 630090, Novosibirsk, Russia
[2]HSE University, 101000, Moscow, Russia
[3]Lebedev Physical Institute of the Russian Academy of Sciences, Troitsk Branch, 108840, Moscow, Russia
[4]School of Physics and Engineering, ITMO University, 197101, St. Petersburg, Russia.
[5]Skolkovo Institute of Science and Technology, 30/1 Bolshoy Boulevard, 121205 Moscow, Russia
[6]Institute of Spectroscopy of the Russian Academy of Sciences, 108840, Moscow, Russia
[7]Moscow Pedagogical State University (MPGU), 119435, Moscow, Russia

Supplementary Note 1: STEM images of the studied PNCs

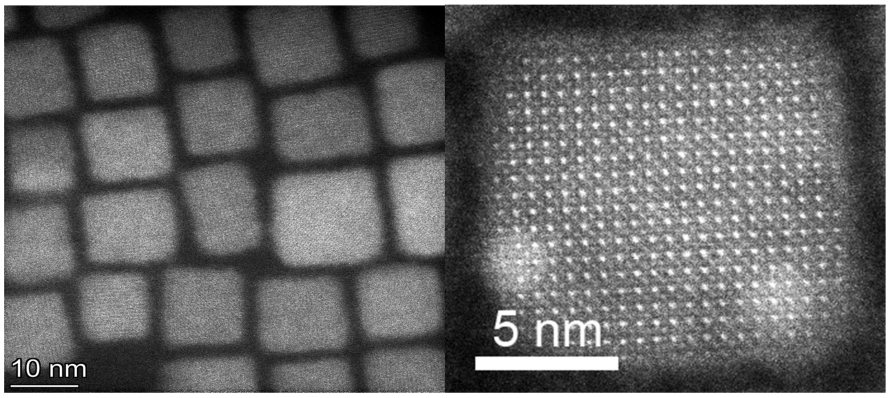

Figure S1: Left panel: STEM image of the ensemble of $CsPbBr_3$ PNCs. Right panel: STEM image of a single PNC.

Supplementary Note 2: Obtaining two-dimensional distributions

To obtain two-dimensional distributions, we divided the range of PL intensities (number of photon counts per bin) into levels numbered with index m. The PL intensity of the m-th level is N_m. The number of levels depends on the maximum PL intensity. Typically one level has a width of two to three photons per bin. The detected photons corresponding to each level were then divided into groups containing 1000 photons each. The set of photon delay times of each group (m, j) is used to calculate the PL decay curve. In this way, one can obtain a set of PL decay curves, each of them is a numerical sequence $N_i^{(m,j)}$, where $N_i^{(m,j)}$ is the number of photon counts with delay time within the i-th time bin. The i-th time bin is defined as time interval between $t_i \equiv i\delta t$ and t_{i+1}, where δt is the width of the time bin. We assume the PL decay to have a biexponential form with background noise for any given set (m, j):

$$w_i(a, \tau_F, \tau_D, b) = A\left(\frac{1}{\tau_F}e^{-t_i/\tau_F} + \frac{a}{\tau_D}e^{-t_1/\tau_D} + b\right) \tag{1}$$

where w_i is the probability of detecting a photon within the i-th bin, a is a relative intensity of the delayed component, and b is the background level. The coefficient A is determined as:

$$A^{-1} = \sum_i \left(\frac{1}{\tau_F}e^{-t_i/\tau_F} + \frac{a}{\tau_D}e^{-t_1/\tau_D} + b\right)$$

Thus, w_i satisfies the normalization condition:

$$\sum_i w_i(a, \tau_F, \tau_D, b) = 1. \tag{2}$$

To estimate the parameters a, τ_F, τ_D, and b, we applied the likelihood function for each group (m, j) using the multinomial distribution as follows:

$$\ln L^{(m,j)}(a, \tau_F, \tau_D, b) = \sum N_i^{(m,j)} \ln w_i(a, \tau_F, \tau_D, b) + const \tag{3}$$

We have found the minima of the negative likelihood function logarithm Eq.(3) using the MATLAB fminsearch function. The resulting estimated parameters are denoted as $a^{(m,j)}$, $\tau_F^{(m,j)}$, $\tau_D^{(m,j)}$, and $b^{(m,j)}$. Estimated PL intensities of the fast and delayed component are

$$N_F^{(m,j)} = N_m Q_F\left(a^{(m,j)}, \tau_F^{(m,j)}, \tau_D^{(m,j)}, b^{(m,j)}\right)$$

$$N_D^{(m,j)} = N_m Q_D\left(a^{(m,j)}, \tau_F^{(m,j)}, \tau_D^{(m,j)}, b^{(m,j)}\right)$$

where

$$Q_F(a, \tau_F, \tau_D, b) = \sum_i A\frac{1}{\tau_F}e^{-t_i/\tau_F}$$

$$Q_D(a, \tau_F, \tau_D, b) = \sum_i A \frac{a}{\tau_D} e^{-t_i/\tau_D}$$

We assume that the maximum value of $N_F^{(m,j)} + N_D^{(m,j)}$ for all groups

$$N_{\max} = \max_{m,j} (N_F^{(m,j)} + N_D^{(m,j)})$$

corresponds to a PL quantum yield of unity. Then, the PL quantum yields of the fast and slow components can be estimated as

$$Y_F^{(m,j)} = \frac{N_F^{(m,j)}}{N_{\max}}, \; Y_D^{(m,j)} = \frac{N_D^{(m,j)}}{N_{\max}} \tag{4}$$

Finally, we get four parameter estimations $\tau_F^{(m,j)}$, $\tau_D^{(m,j)}$, $Y_F^{(m,j)}$, and $Y_D^{(m,j)}$ for each group of photons. This allows us to obtain four different two-dimensional distributions $\rho_1(\tau_F, \tau_D)$, $\rho_2(\tau_F, Y_F)$, $\rho_3(\tau_D, Y_D)$ and $\rho_4(Y_D + Y_F, Y_F)$, which are presented in Fig. 4 in the main text and in the Supplementary Note 6.

Supplementary Note 3: Estimation of the biexciton lifetime

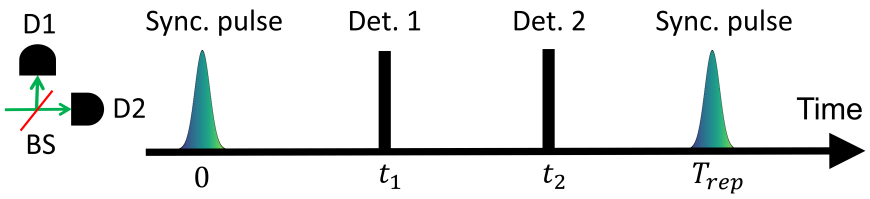

Figure S2: Schematic picture of pair detection after the one pulse excitation

To estimate the biexciton lifetime, we only collected events when both detectors in the Hanbury Brown and Twiss scheme were triggered as a result of a single excitation pulse. The schematic picture of such an event is presented in Fig. S2: two photons are registered on different detectors. Denoting the smallest of time delays (the first photon delay time) as t_1, one can obtain the decay curve as a numerical sequence N_i^{XX}, where N_i^{XX} is the number of first photons delay times within the i-th time bin. This distribution can be fitted with the biexponential decay law Eq.(1) in the same manner as was done in the Supplementary Note 2. An example of the t_1 normalized distribution

$$p_i^{XX} = \frac{N_i^{XX}}{\sum\limits_k N_i^{XX}} \tag{5}$$

and its fit is presented in Fig. 5a in the main text.

Supplementary Note 4: Analytical solution for excitation relaxation kinetics

The kinetic mechanism of the excitation relaxation proposed in the main article (Fig. 6) is described by the following set of equations:

$$\begin{cases} \frac{dp_e}{dt} = -(k_r + k_n + k_t)p_e + k_d p_t \equiv -\Gamma_e p_e + k_d p_t \\ \frac{dp_t}{dt} = -(k'_r + k'_n + k_d)p_t + k_t p_e \equiv -\Gamma_t p_e + k_t p_e \end{cases} \tag{6}$$

with the initial conditions:

$$p_e(0) = p_0, \quad p_t(0) = 1 - p_0 \tag{7}$$

The system Eq.(6) can be written in matrix form:

$$\frac{d}{dt}\begin{pmatrix} p_e(t) \\ p_t(t) \end{pmatrix} = \hat{\boldsymbol{M}}\begin{pmatrix} p_e(t) \\ p_t(t) \end{pmatrix} \tag{8}$$

where:

$$\hat{\boldsymbol{M}} = \begin{pmatrix} -\Gamma_e & k_d \\ k_t & -\Gamma_t \end{pmatrix}$$

The eigenvalues of the matrix $\hat{\boldsymbol{M}}$ are solutions of the following equation:

$$\det\left(\hat{\boldsymbol{M}} - \lambda\hat{\boldsymbol{E}}\right) = \lambda^2 + \lambda(\Gamma_e + \Gamma_t) + (\Gamma_e\Gamma_t - k_t k_d) = 0 \tag{9}$$

where $\hat{\boldsymbol{E}}$ is the unity matrix. Solving Eq.(9), we obtain two eigenvalues:

$$\lambda_{F,D} \equiv -\frac{1}{\tau_{F,D}} = -\frac{1}{2}\left[(\Gamma_e + \Gamma_t) \pm |\Gamma_e - \Gamma_t|\sqrt{1 + \frac{4k_t k_d}{(\Gamma_e - \Gamma_t)^2}}\right]. \tag{10}$$

That corresponds to Eq. (6) in the main text for fast and delayed component times. The equation for eigenvectors is as follows:

$$\left(\hat{\boldsymbol{M}} - \lambda_{F,D}\hat{\boldsymbol{E}}\right)\vec{\boldsymbol{X}}_{1,2} = 0. \tag{11}$$

The solutions are as follows:

$$\vec{\boldsymbol{X}}_1 = \begin{pmatrix} X_1 \\ 1 \end{pmatrix}; \quad \lambda = \lambda_F, \tag{12}$$

$$\vec{\boldsymbol{X}}_2 = \begin{pmatrix} X_2 \\ 1 \end{pmatrix}; \quad \lambda = \lambda_D, \tag{13}$$

where:

$$X_1 = 2k_d\left[(\Gamma_e - \Gamma_t) - |\Gamma_e - \Gamma_t|\sqrt{1 + \frac{4k_t k_d}{(\Gamma_e - \Gamma_t)^2}}\right]^{-1},$$

$$X_2 = 2k_d \left[(\Gamma_e - \Gamma_t) + |\Gamma_e - \Gamma_t| \sqrt{1 + \frac{4k_t k_d}{(\Gamma_e - \Gamma_t)^2}} \right]^{-1}.$$

A general solution of Eq.(8) is a sum of two vectors:

$$\begin{pmatrix} p_e(t) \\ p_t(t) \end{pmatrix} = C_F \begin{pmatrix} X_1 \\ 1 \end{pmatrix} e^{-t/\tau_F} + C_D \begin{pmatrix} X_2 \\ 1 \end{pmatrix} e^{-t/\tau_D}, \tag{14}$$

where C_1 and C_2 are unknown constants that can be found using the initial conditions (7). The solution for the coefficients is as follows:

$$C_F = \frac{X_2(1-p_0) - p_0}{X_2 - X_1}, \tag{15}$$

$$C_D = \frac{p_0 - X_1(1-p_0)}{X_2 - X_1}. \tag{16}$$

PL decay curve is given by the following expression:

$$p(t) = k_r p_e(t) + k'_r p_t(t) \tag{17}$$

Finally we obtain expressions for the quantum yields:

$$Y_F = C_F \tau_F (k_r X_1 + k'_r), \quad Y_D = C_D \tau_D (k_r X_2 + k'_r) \tag{18}$$

The total quantum yield of PL emission is defined as

$$Y = Y_F + Y_D \tag{19}$$

The function $p(t)$, characteristic times τ_F, τ_D and quantum yields Y_F, Y_D, and Y are determined by the values of the kinetic parameters

$$k_r, k'_r, k_n, k'_n, k_t, k_d, p_0$$

Supplementary Note 5. Fitting procedure

Fitting the PL decay kinetics

From the PL intensity levels defined in the Supplementary Note 2, we selected seven equally spaced levels with indices m_k, where $k = 1 \dots 7$. We will denote $(k) \equiv m_k$. We collected photon delay times within each level and obtained seven PL decay curves $N_i^{(k)}$. Then we defined the likelihood function for each level according to the multinomial distribution:

$$\ln l^{(k)}\left(\vec{\boldsymbol{\nu}}, S_k\right) = \ln C^{(k)} + \sum_i N_i^{(k)} \ln w_i^{(k)}\left(\vec{\boldsymbol{\nu}}, S_k\right), \tag{20}$$

where $C^{(k)}$ is the multinomial coefficient:

$$C^{(k)} \equiv \binom{\sum_i N_i^{(k)}}{N_1^{(k)} N_2^{(k)} \dots N_{i_m}^{(k)}} = \frac{\left(\sum_i N_i^{(k)}\right)!}{N_1^{(k)}! \dots N_{i_m}^{(k)}!}$$

The b_k parameter describes the level of background emission, $w_i^{(k)}$ is the theoretical distribution of probabilities

$$w_i^{(k)}\left(\vec{\boldsymbol{\nu}}, b_k\right) = \frac{p\left[\vec{\boldsymbol{\nu}}, S_k\right](t_i) + b_k}{\sum_i \left(p\left[\vec{\boldsymbol{\nu}}, S_k\right](t_i) + b_k\right)} \tag{21}$$

$\vec{\boldsymbol{\nu}}$ is the vector containing the fitting parameters

$$\vec{\boldsymbol{\nu}} = (k_r, k_r', k_0, k_0', k_t, p_0, \Delta E)$$

The Huang-Rhys parameter for the (k)-th level S_k is found by solving the following equation:

$$Y\left[\vec{\boldsymbol{\nu}}, S_k\right] = \frac{N_{(k)}}{N_M} \tag{22}$$

$p\left[\vec{\boldsymbol{\nu}}, S\right](t)$ and $Y\left[\vec{\boldsymbol{\nu}}, S\right]$ are the PL decay function Eq.(17) and the total quantum yield Eq.(19), respectively, with the following parameters:

$$k_r, k_r', k_n = k_0 S^{\alpha}, k_n' = k_0' S^{\alpha'}, k_t, k_d = k_t \exp(-\Delta E / k_B T), p_0$$

The total likelihood function is as follows:

$$\ln L\left(\vec{\boldsymbol{\nu}}, \vec{\boldsymbol{b}}\right) = \sum_{k=1}^{7} \ln l^{(k)} = \sum_{k=1}^{7} \left(\ln C^{(k)} + \sum_i N_i^{(k)} \ln w_i^{(k)}\left(\vec{\boldsymbol{\nu}}, b_k\right)\right) \tag{23}$$

where $\vec{\boldsymbol{b}}$ is the vector containing b_k values. The fitting parameters $\vec{\boldsymbol{\nu}}$ and $\vec{\boldsymbol{b}}$ estimations were found by searching for the minimum negative value of the likelihood function logarithm using the MATLAB fminsearch function. Eq.(22) was solved numerically for every step of the fitting procedure using the MATLAB fminserch function.

Using the estimated parameters, the theoretical Huang-Rhys parameter dependencies of $\tau_F(S)$, $\tau_D(S)$, $Y_F(S)$, $Y_D(S)$ and $Y(S)$ were calculated. As a result, we obtain theoretical dependencies $\tau_F - \tau_D$, $\tau_F - Y_F$, $\tau_D - D$ and $Y - Y_F$. These dependencies are shown in Fig. 8 of the main article as red lines.

Fitting PSD and PDF

The theoretical calculations of the power spectral density (Eq. (15) in the main article) and the photon distribution function (Eq. (16) in the main article) within the proposed model were performed according to the procedure described in detail in the Ref. 1 Supplementary notes 8 and 9. The procedure used the theoretical dependence of the quantum yield on the Huang-Rhys parameter $Y[\vec{\boldsymbol{\nu}}, S]$, given by Eq.(19), which differs from the dependence used in Ref. 1. Fitting of the estimated PSD and PDF was performed according to the procedure described in detail in the Ref. 1 Supplementary note 10.

Error estimation for two-dimensional distributions

The mean values of $\tau_{F,D}$, $Y_{F,D}$, and Y over a time bin, which had a starting system configuration of Σ, can be found as (see the Ref. 1 Supplementary note 11):

$$\overline{\tau}_{F,D}(\Sigma) = \sum_{\Sigma'} \tau_{F,D}(\Sigma') \overline{G}_{\Sigma'\Sigma} \tag{24}$$

$$\overline{Y}(\Sigma) = \sum_{\Sigma'} Y_{\Sigma'} \overline{G}_{\Sigma'\Sigma}; \quad \overline{Y}_{F,D}(\Sigma) = \sum_{\Sigma'} Y_{F,D}(\Sigma') \overline{G}_{\Sigma'\Sigma} \tag{25}$$

where

$$\overline{G}_{\Sigma'\Sigma} = \frac{1}{\Delta} \int_0^{\Delta t} G_{\Sigma'\Sigma}(t)\, dt$$

and

$$\tau_{F,D}(\Sigma) \equiv \tau_{F,D}(S(\Sigma)); \quad Y_{F,D}(\Sigma) \equiv Y_{F,D}(S(\Sigma))$$

The mean number of detected photons per time bin is

$$\overline{N}_\Sigma = N_{\max} \overline{Y}(\Sigma)$$

The probability to detect k photons within the bin is

$$P_\Sigma(k) = \frac{\overline{N}_\Sigma^k}{k!} \exp\left(-\overline{N}_\Sigma\right)$$

We chose bins that had a number of detected photons k within level m, so $N_m \le k < N_{m+1}$. The prior probability of the configuration Σ is $P_{st}(\Sigma)$. The

posterior Bayes probability when k is within the m-th level is

$$P_m(\Sigma) = \frac{\sum\limits_{N_m \le k < N_{m+1}} P_\Sigma(k) P_{st}(\Sigma)}{\sum\limits_{N_m \le k < N_{m+1}} PDF(k)} \tag{26}$$

The mean value of the PL quantum yield for the m-th level bin is

$$\overline{Y}_m = \sum_\Sigma \overline{Y}_\Sigma P_m(\Sigma)$$

and the variance of Y_m is

$$\mathrm{Var}\left[\overline{Y}_m\right] = \sum_\Sigma \overline{Y}_\Sigma^2 P_m(\Sigma) - \overline{Y}_m^2 \tag{27}$$

Recall that the estimations of the $\tau_{F,D}$ and $Y_{F,D}$ are calculated using the maximum likelihood method for multinomial distribution. We will consider the special case of $\delta t \ll \tau_F$ and $T_{rep} \gg \tau_D$. The probability density is as follows:

$$w_\theta(t) = \frac{Q_F}{\tau_F} e^{-t/\tau_F} + \frac{Q_D}{\tau_D} e^{-t/\tau_D} \tag{28}$$

where $Q_D = 1 - Q_F$ and $\vec{\boldsymbol{\theta}}$ is the vector parameter

$$\vec{\boldsymbol{\theta}} = (\tau_F, \tau_D, Q_F)$$

We also neglect background noise. The variance of an unbiased estimator of any parameter θ_i obtained from the maximum likelihood method obeys the Cramer–Rao bound (see Ref. 2 for example):

$$\sigma_{\theta_i}^2 \ge \left[\hat{\boldsymbol{F}}^{-\mathbf{1}}\right]_{ii} \tag{29}$$

where $\hat{\boldsymbol{F}}$ is the Fisher's information matrix with elements:

$$F_{ij} = N_p \int_0^\infty \frac{1}{w_\theta(t)} \left(\frac{\partial w_\theta(t)}{\partial \theta_i}\right) \left(\frac{\partial w_\theta(t)}{\partial \theta_j}\right) dt \tag{30}$$

where N_p is the total number of counts in a single PL decay curve. The partial derivatives of the probability density are given by:

$$\frac{\partial w_\theta(t)}{\partial Q_F} = \frac{1}{\tau_F} e^{-t/\tau_F} - \frac{1}{\tau_D} e^{-t/\tau_D}$$

$$\frac{\partial w_\theta(t)}{\partial \tau_{F,D}} = \frac{Q_{F,D}}{\tau_{F,D}^2} e^{-t/\tau_{F,D}} \left(\frac{t}{\tau_{F,D}} - 1\right)$$

Substituting these expressions into Eqs. (29-30), one can obtain the variances of the parameters' estimators $\sigma^2_{\tau_F}$, $\sigma^2_{\tau_D}$, and $\sigma^2_{Q_F}$. We have calculated these values using the numerical integration for each configuration Σ by setting

$$\tau_{F,D} = \tau_{F,D}(\Sigma); \quad Q_F(\Sigma) = Y_F(\Sigma)/Y(\Sigma)$$

The obtained values are denoted as $\sigma^2_{\theta_i}(\Sigma)$. After averaging the variances of the parameters over the configurations at the beginning of the bin and over the fluctuations within the bin, we obtain the total variances at the level m :

$$\overline{\sigma^2_{\theta_i}} = \sum_{\Sigma} \sum_{\Sigma'} \sigma^2_{\theta_i}(\Sigma') \overline{G}_{\Sigma'\Sigma} P_m(\Sigma) \tag{31}$$

The variance for characteristic times at level m can be then found as:

$$\mathrm{Var}_m[\tau_{F,D}] = \overline{\sigma^2_{\tau_{F,D}}} \tag{32}$$

The estimators of $Y_{F,D}$ are the products of two independent estimators:

$$Y_{F,D} = Q_{F,D} \overline{Y}_m \tag{33}$$

Thus, the total variance for $Y_{F,D}$ at level m can be calculated as:

$$\mathrm{Var}_m[Y_{F,D}] = \bar{Y}^2_m \overline{\sigma^2_{Q_F}} + Q^2_{F,D} \mathrm{Var}\left[\overline{Y}_m\right] \tag{34}$$

The calculated 3σ confidence regions for the two levels are shown in Fig. 8 of the main article as yellow ellipses.

Supplementary Note 6. Trapping rate calculations.

In this section, we consider the applicability of the proposed approximation for the rate constant of the non-radiative capture into a deep trap:

$$k_n = k_0 S^{\alpha} \tag{35}$$

It is well known that the rate of non-radiative transfer of an electron to a deep trap with the emission of multiple optical phonon quanta is described by the Marcus-Jortner formula (see, for example [3]):

$$k_n = \frac{2\pi|V|^2}{\hbar}\sqrt{\frac{1}{4\pi\lambda_{ac}kT}}\sum_{n=-\infty}^{n=\infty} P_n \exp\left(-\frac{(\delta E + \lambda_{ac} + n\hbar\omega_{LO})^2}{4\lambda_{ac}kT}\right) \tag{36}$$

where V is the electron coupling matrix element, λ_{ac} is the reorganization energy of the classical modes. P_n is the probability to emit n phonon quanta during the transition:

$$P_n = I_n\left(\frac{S}{\sinh\tilde{\omega}}\right)\exp\left(n\tilde{\omega} - S\coth\tilde{\omega}\right) \tag{37}$$

where I_n is the modified Bessel function of the n-th order and $\tilde{\omega} = \hbar\omega_{LO}/(2kT)$. Within the low-temperature limit $\tilde{\omega} \gg 1$, this expression tends to the Poisson distribution:

$$P_n = \frac{S^n}{n!}e^{-S} \tag{38}$$

As shown in Fig. S3, the S dependence of the trapping rate approximation Eq.(35) with parameter values obtained from the fitting procedure for the NC described in the main text, *i.e.* $k_0 = 7.54\times10^5$ ns^{-1} and $\alpha = 10$ coincides with the Marcus-Jortner formula for $S \ll 1$. The parameters of the electron transfer are: the LO phonons' energy $\hbar\omega_{LO} = 17$ meV, the electron coupling matrix element $V = 51$ meV, the deep trap energy $\delta E = -170.1$ meV. The electronic coupling value is quite typical for single quantum dots and nanocrystals, the ratio $|\delta E|/\hbar\omega_{LO} = 10.006$ is also in the agreement with the approximation.

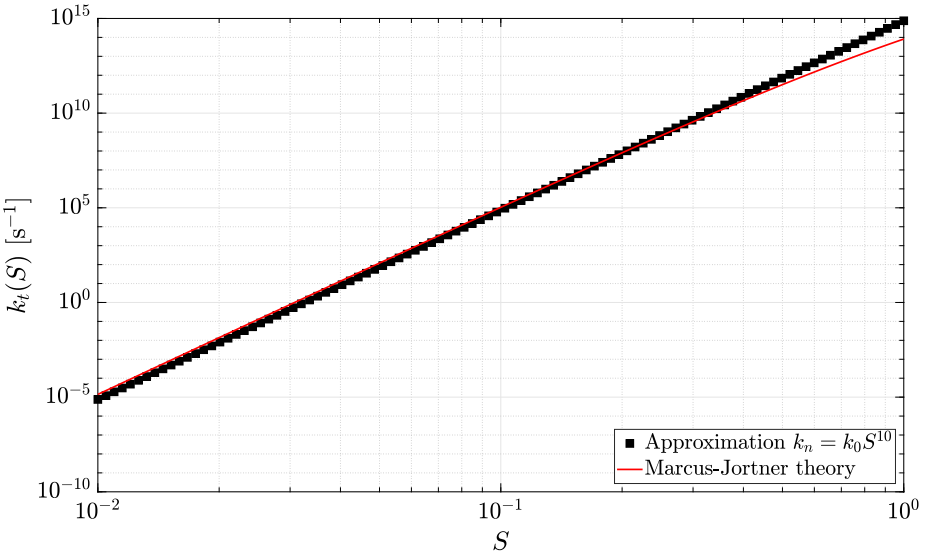

Figure S3: Carrier trapping rate constant dependence on Huang-Rhys parameter using approximation $k_n = k_0 S^{10}$ (black squares) and its fit with the Marcus-Jortner formula (red line). Fit parameters are δE = -170.1 meV, V = 51 meV, λ_{ac} = 0.1 meV

Supplementary Note 7. Processing results for the studied PNCs

Figures S4 - S9 present the processing results for the studied PNCs. All figures have the same structure.
Panel (a) represents the PL intensity blinking trace. Panel (b) shows a photon distribution function with a theoretical fit (red line).
Panels (c), (d), (f), and (g) represent the four two-dimensional distributions described in the previous sections with corresponding fits (red lines).
Panel (e) shows the photon cross-correlation function on short times, normalized to the maximum. The value of $g^{(2)}(0)$ is indicated in each figure.
Panel (h) shows the first photon delay time characteristics, obtained according to the procedure described in the Supplementary Note 3. Note that the panel shows the survival probability, not the distribution function Eq.(5) presented in Fig. 5a in the main text. The survival probability is defined as

$$S_i^{XX} = 1 - \frac{\sum_{k=0}^{i} N_i^{XX}}{\sum_{k} N_i^{XX}} \tag{39}$$

Panel (h) shows the guide-to-eye exponential decay function (red line). The characteristic time is indicated in each figure.
Panel (i) shows the integrated PL decay.
Panel (j) presents the estimated power spectral density with its corresponding theoretical fit (red line).
Panel (k) shows the long-term correlation function of the PL intensity.

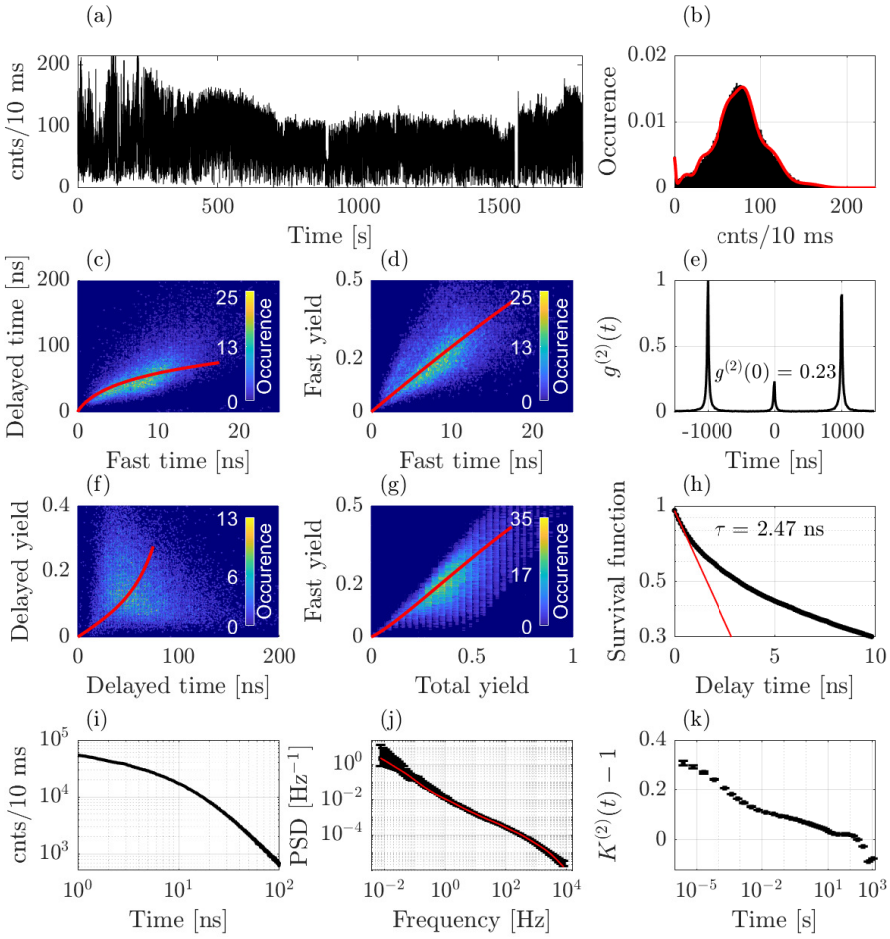

Figure S4: PNC #1

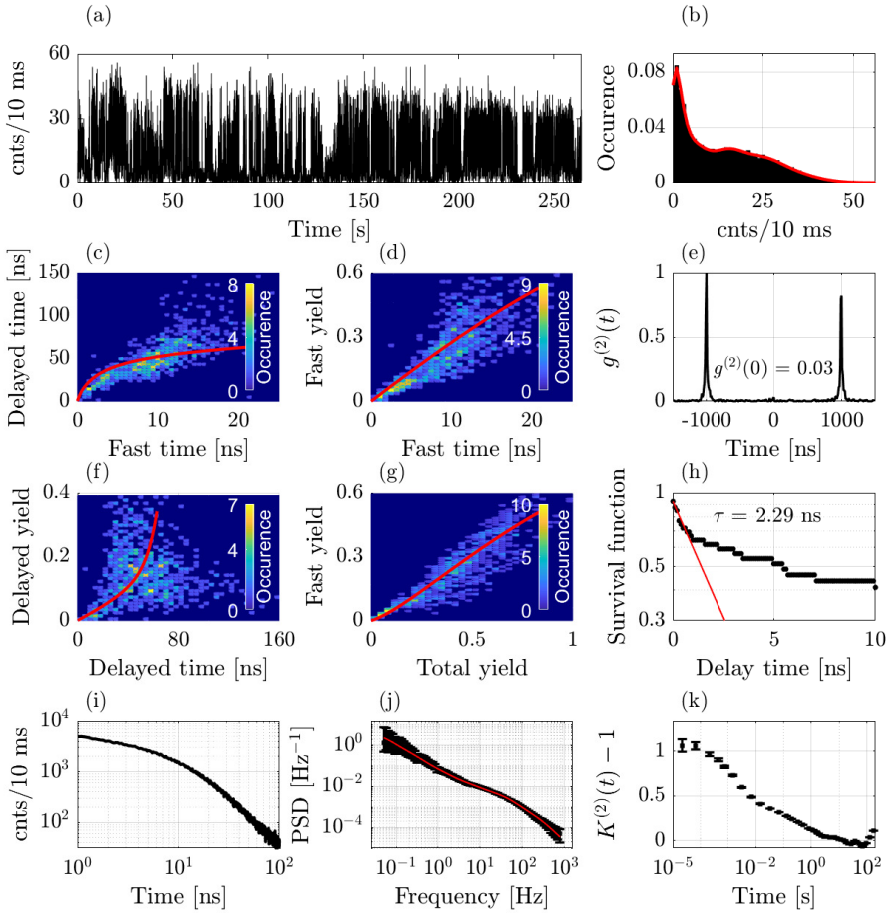

Figure S5: PNC #2

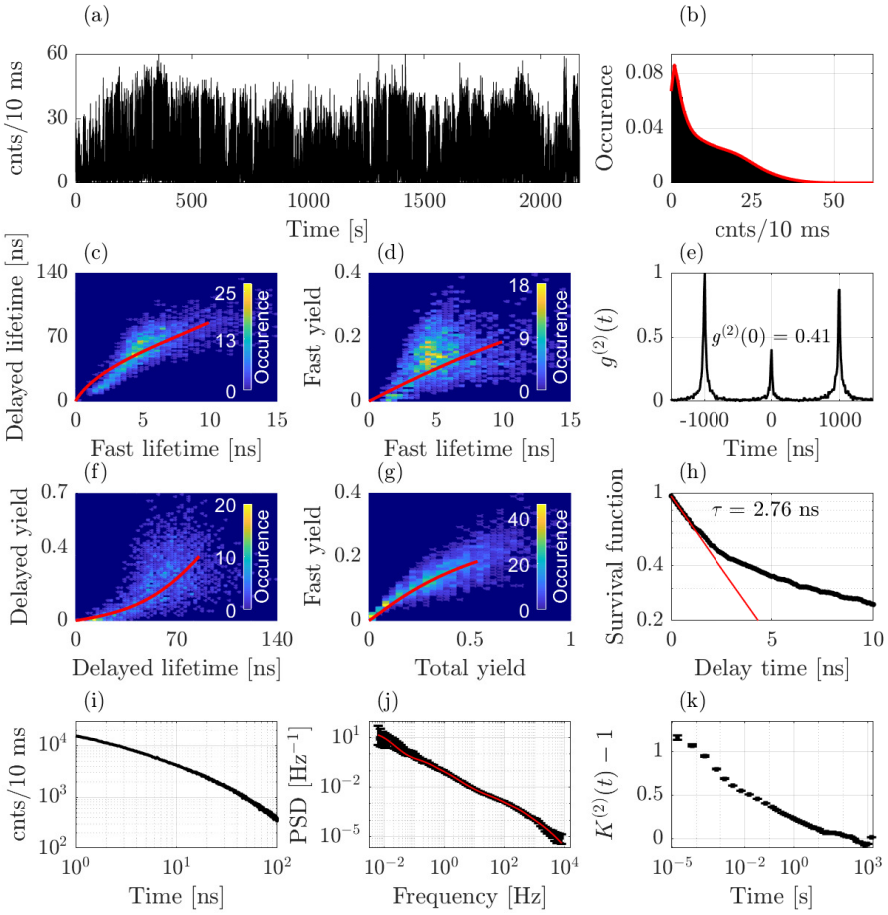

Figure S6: PNC #3

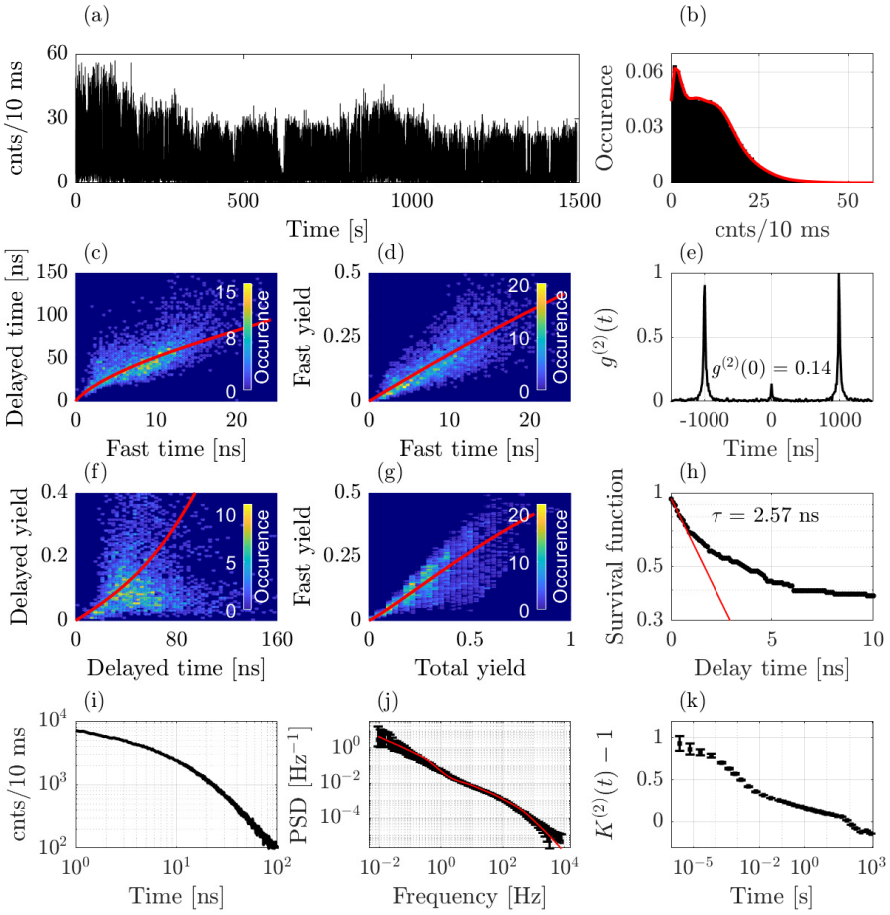

Figure S7: PNC #4

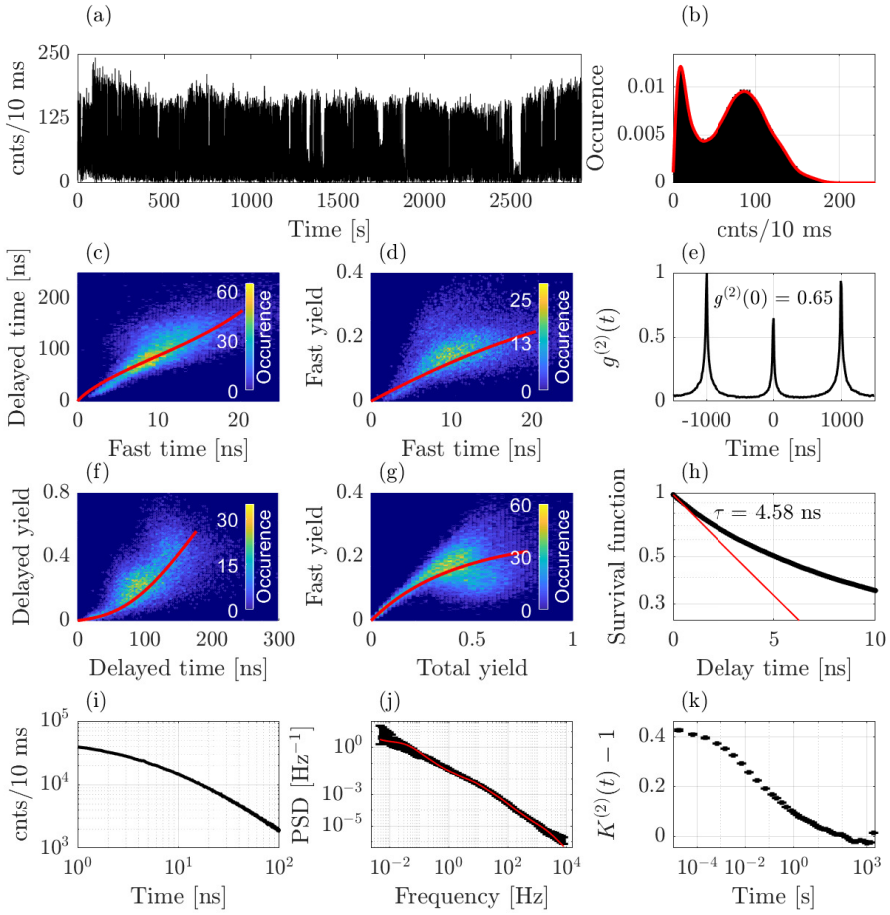

Figure S8: PNC #5. The results for this PNC are presented in the main article.

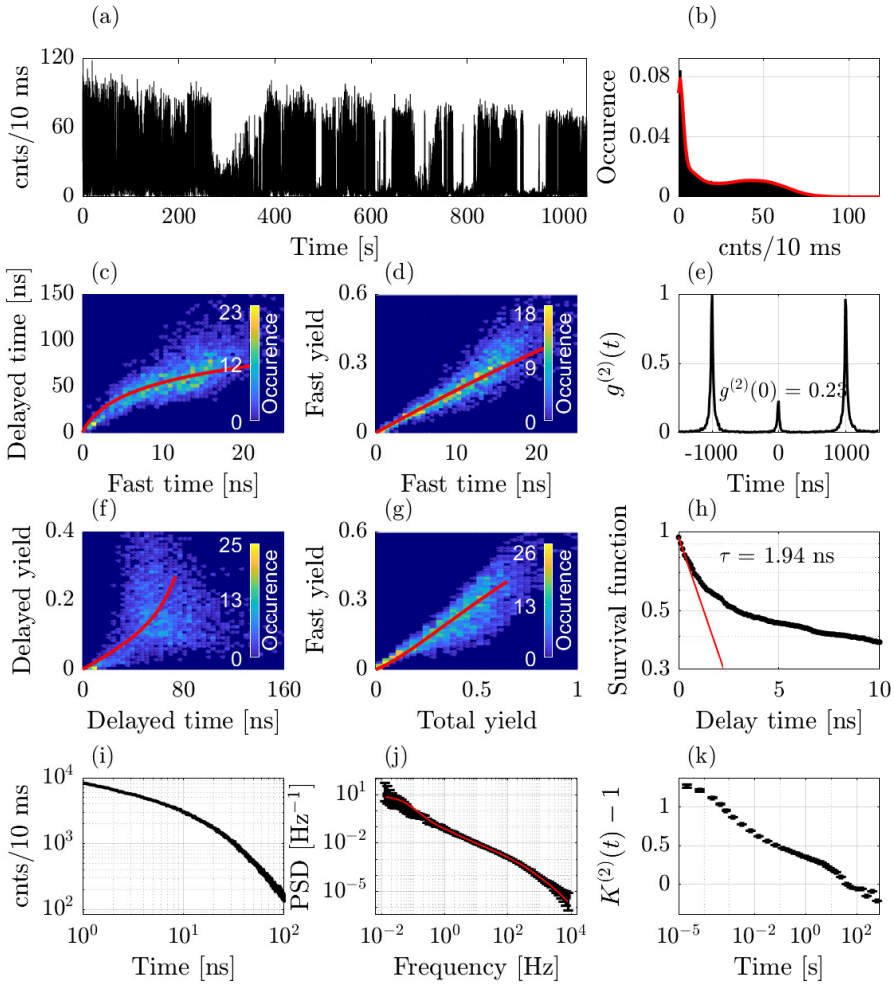

Figure S9: PNC #6

Supplementary Note 8. Model parameters obtained from fitting procedures.

	PNC number					
	#1	#2	#3	#4	#5	#6
k_r [ns^{-1}]	0.0325	0.343	0.0431	0.0286	0.0265	0.0238
k_r' [ns^{-1}]	0.0095	0.0133	0.0025	0.0074	0.0011	0.0103
k_t [ns^{-1}]	0.0065	0.0069	0.0210	0.0057	0.0145	0.0048
k_0 [ns^{-1}]	5.64 $\times 10^5$	3.37 $\times 10^5$	7.06 $\times 10^5$	3.52 $\times 10^5$	7.54 $\times 10^5$	5.42 $\times 10^5$
k_0' [ns^{-1}]	4.3 $\times 10^3$	2.05 $\times 10^3$	5.84 $\times 10^3$	5.29 $\times 10^3$	8.13 $\times 10^3$	3.96 $\times 10^3$
ΔE [meV]	25.77	25.07	22.99	25.45	21.97	27.20
p_0	0.788	0.837	0.501	0.6659	0.5	0.7977
s_0	0	0.0326	0.0844	0	0.0349	0.0196
s_1	0.0121	—	0.0211	0.0262	0.0097	—
s_2	0.0577	—	—	—	0.0149	0.1159
s_3	0.0254	0.0206	0.0676	0.0289	—	0.0203
s_4	0.0184	0.1280	—	0.1157	0.0567	0.1039
s_5	0.2667	0.0504	0.0587	0.0650	0.0198	0.0885
s_6	0.0766	0.1243	0.0391	—	0.1028	0.0451
s_7	0.0450	0.0367	0.0281	0.1791	0.0551	0.0458
s_8	0.0199	0.1354	0.0749	0.0380	0.0203	0.0735
s_9	0.0587	0.0537	0.0742	0.0503	0.0956	0.0848
s_{10}	0.0470	—	0.0743	0.0642	0.0925	0.0861
p_1	0.4218	—	0.6027	0.4477	0.453	—
p_2	0.0398	—	—	—	0.353	0.7418
p_3	0.194	0.6054	0.3559	0.7497	—	0.3583
p_4	0.6883	0.2852	—	0.9866	0.206	0.4254
p_5	0.0098	0.3374	0.8660	0.2308	0.689	0.9737
p_6	0.9832	0.0876	0.4701	—	0.9777	0.5316
p_7	0.9678	0.6663	0.6008	0.0846	0.124	0.5512
p_8	0.4667	0.9178	0.1599	0.5823	0.470	0.2190
p_9	0.0891	0.2467	0.2000	0.8456	0.016	0.1696
p_{10}	0.921	—	0.091	0.024	0.020	0.0573
Γ_1 [s^{-1}]	1.6×10^{-3}	—	1.6×10^{-3}	1.6×10^{-3}	1.6×10^{-3}	—
Γ_2 [s^{-1}]	9.3×10^{-3}	—	—	—	9×10^{-3}	9×10^{-3}
Γ_3 [s^{-1}]	5.4×10^{-2}	5.4×10^{-2}	5.4×10^{-2}	5.4×10^{-2}	—	5.4×10^{-2}
Γ_4 [s^{-1}]	3.2×10^{-1}	3.2×10^{-1}	—	3.2×10^{-1}	2.9×10^{-1}	2.9×10^{-1}
Γ_5 [s^{-1}]	1.8 $\times 10^0$	1.8 $\times 10^0$	1.8 $\times 10^0$	1.8 $\times 10^0$	1.6 $\times 10^0$	1.6 $\times 10^0$
Γ_6 [s^{-1}]	10.8 $\times 10^0$	10.8 $\times 10^0$	10.8 $\times 10^0$	—	9.5×10^0	9.5×10^0
Γ_7 [s^{-1}]	6.3 $\times 10^1$	6.3 $\times 10^1$	6.3 $\times 10^1$	6.3 $\times 10^1$	5.4×10^1	5.4×10^1
Γ_8 [s^{-1}]	3.7×10^2	3.7×10^2	3.7×10^2	3.7×10^2	3.1×10^2	3.1×10^2
Γ_9 [s^{-1}]	2.15×10^3	2.15×10^3	2.15×10^3	2.15×10^3	1.8×10^3	2.27×10^3
Γ_{10} [s^{-1}]	1.26×10^4	—	1.26×10^4	1.26×10^4	1×10^4	1×10^4

Supplementary Note 9. Single PNC's emission spectra.

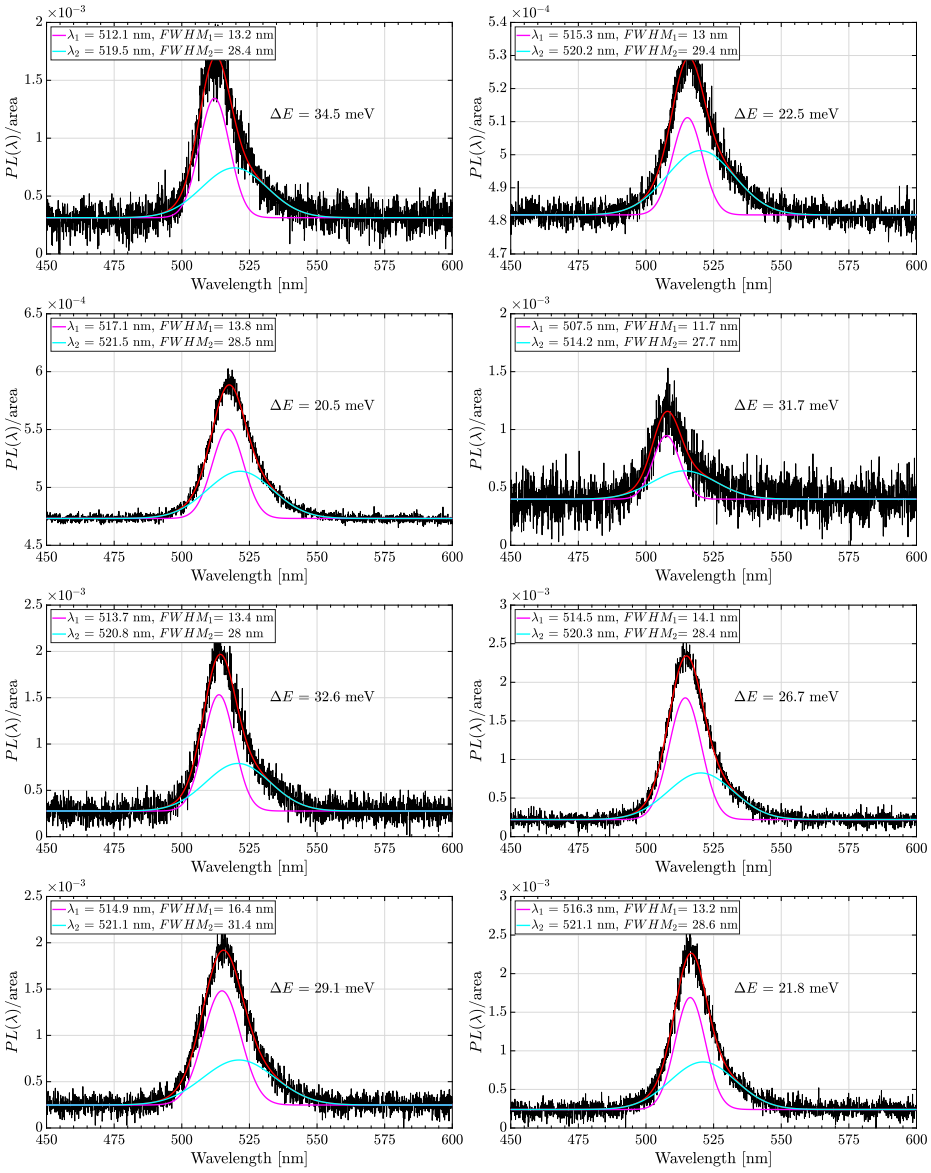

Figure S10: Experimental emission spectra of the single PNC (black line) and its fit using two gaussians (red line). Short wavelength and long wavelength components are marked with magenta and cyan lines, respectively.

Supplementary Note 10. PDF and PSD calculations within the MRC model.

The standard MRC model[4] is based on the trapping mechanism of blinking. The trapping rate within the model is defined as follows:

$$k_t(t) = k_0 + \sum_{i=1}^{N} \sigma_i(t) k_i \tag{40}$$

where k_i is the trapping rate for the i-th recombination center (RC) and $\sigma_i(t)$ is a random function of time switching between two values 1 (i-th RC is ON) and 0 (i-th RC is OFF). The quantum yield for each configuration Σ is as follows:

$$Y_\Sigma = \frac{1}{1 + k_t(\Sigma)/k_r} \tag{41}$$

In the Ref. [1] we put forward the argument why the MRC model cannot explain the extremely low values of the PL quantum yield (<1%) observed in the experiment. In order to reproduce $1/f$ form of the PL intensity power spectral density, one has to set all trapping rates k_i approximately the same values. To reproduce a nearly continuous photon distribution function, k_i has to be of the same order as k_r. Thus, the minimal PL quantum yield within MRC model is

$$Y_{\text{low}} = \frac{1}{1 + \left(k_0 + \sum\limits_{i=1}^{N} k_i\right)/k_r} \approx \frac{1}{N+1} \tag{42}$$

To explain the minimal quantum yield in order of ~ 0.01, one has to assume the presence of about a hundred fluctuation recombination centers on the surface of a single QD. The existence of such a large number of recombination centers in an object as small as a nanocrystal seems extremely physically unlikely.

To illustrate this argument, we performed simulations within the MRC model for the standard case, in which all k_i are equal to k_r, and for cases where one of the trapping rates is much larger than the others. The number of recombination centers N was set equal to 10. The characteristic switching times Γ_i were log-uniformly distributed between 10^{-2} and 10^3 s^{-1}. The on γ_i^+ and off γ_i^- rates of each individual RC were equal. The bin time was set to 10 ms. The mean number of counts per bin was set equal to 80. The calculations were performed for 4 values of k_4, starting from $k_4 = k_r$ to $k_4 = 100\ k_r$. The remaining trapping rates k_i were set equal to k_r, $k_0 = 0$. The characteristic switching time for the 4-th RC was $\Gamma_4 = 4.6 \times 10^{-1} s^{-1}$. The PSDs and PDFs were calculated using Eqs.(14-15) and Eq.(16) in the main article, respectively. The results are shown in Figs. S11 and S12.

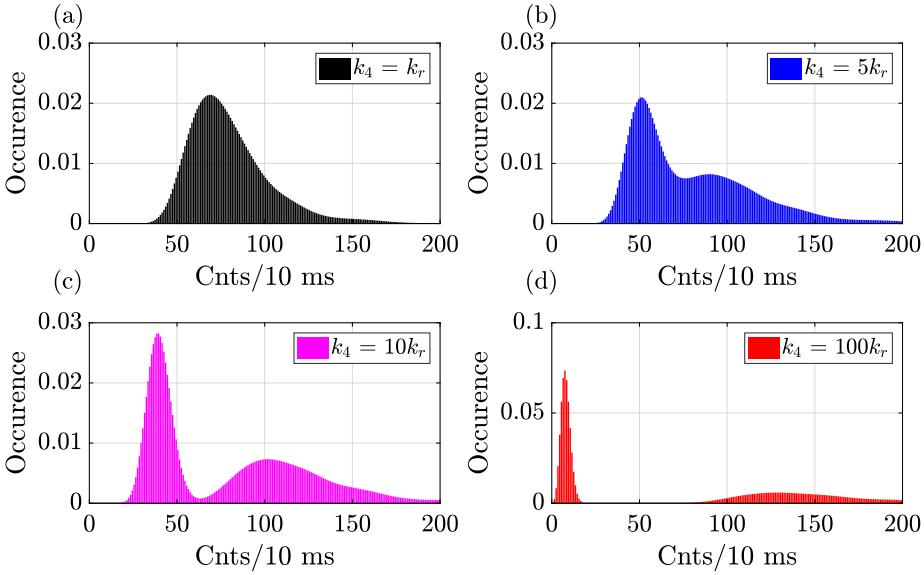

Figure S11: (a-d) Photon distribution function obtained for different values of k_4 within the MRC theory framework (colored bars).

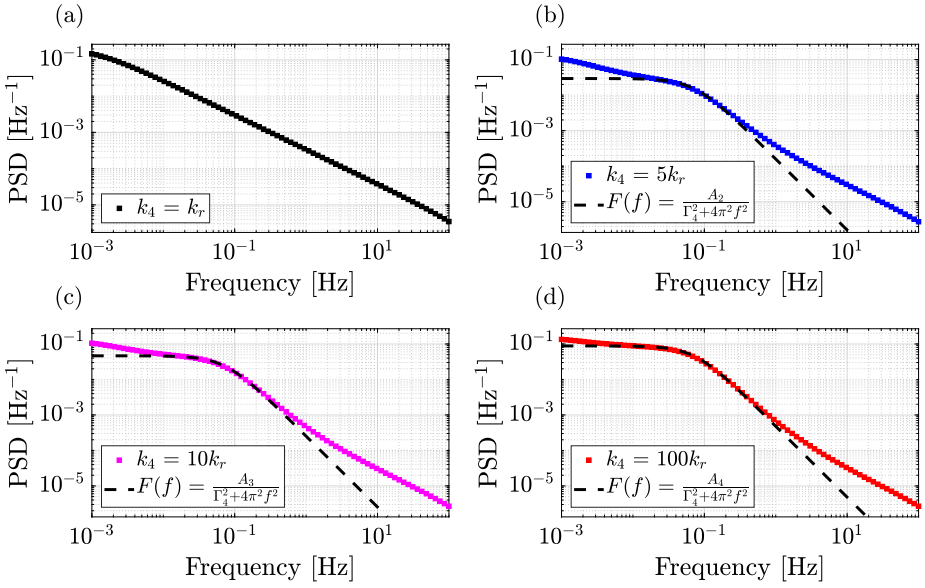

Figure S12: (a-d) Power spectral density obtained for different values of k_4 within the MRC theory framework (solid lines). The dashed lines show the contribution to the PSD from the switching of the fourth recombination center alone.

Figure S12(a) shows that, in the standard case of equal trapping rates, the PSD has a power law form, which corresponds to the experimental observations. The PDF in this case (shown in Fig. S11(a)) is nearly continuous with one broad peak, low PL intensities (with a number of counts per bin less than 30) are absent. In order to achieve the very low PL intensities in the standard case, the number of RCs would have to be increased significantly.

Another way to reduce the minimum PL intensity is to make one or more trapping rates k_i much larger than k_r. Figures S11(b-d) show that increasing the capture rate of one recombination center leads to the appearance of an additional peak in the PDF, which is shifted towards lower intensities. However, even in the extreme case of $k_4 = 100\ k_r$, shown in Fig. S11(d), the peak position does not reach the PL intensity level of 1% from maximum, which is often observed in experiments. As can be concluded from Figs. S12(c-d), increasing the k_4 value leads to a significant deviation of the PSD from the power-law dependence. The dashed lines in these figures show the contribution to the PSD from the switching of the fourth recombination center alone (Lorentzian dependence).

We show that a significant increase in the trapping rates of several recombination centers will lead to the appearance of additional peaks in the PDF and an even greater deviation of the PSD from the power-law dependence, which contradicts the experiment. Therefore, it can be concluded that the MRC theory is not able to adequately describe the blinking properties of a single nanocrystal.

References

[1] E. Podshivaylov, M. Kniazeva, A. Tarasevich, I. Eremchev, A. Naumov and P. Frantsuzov, *Journal of Materials Chemistry C*, 2023, **11**, 8570–8576.

[2] D. Bouchet, V. Krachmalnicoff and I. Izeddin, *Opt. Express*, 2019, **27**, 21239–21252.

[3] A. V. Barzykin, P. A. Frantsuzov, K. Seki and M. Tachiya, in *Solvent Effects in Nonadiabatic Electron-Transfer Reactions: Theoretical Aspects*, John Wiley & Sons, Ltd, 2002, ch. 9, pp. 511–616.

[4] P. A. Frantsuzov, S. Volkán-Kacsó and B. Jankó, *Phys. Rev. Lett.*, 2009, **103**, 207402.